



HAL
open science

Analytical model of a wall acoustic impedance and experimental comparisons

Béatrice Faverjon, Christian Soize

► **To cite this version:**

Béatrice Faverjon, Christian Soize. Analytical model of a wall acoustic impedance and experimental comparisons. Eighth International Conference on Recent Advances in Structural Dynamics (RASD 2003), Jul 2003, Southampton, United Kingdom. pp. 1 - 12. hal-00687877

HAL Id: hal-00687877

<https://hal.science/hal-00687877>

Submitted on 15 Apr 2012

HAL is a multi-disciplinary open access archive for the deposit and dissemination of scientific research documents, whether they are published or not. The documents may come from teaching and research institutions in France or abroad, or from public or private research centers.

L'archive ouverte pluridisciplinaire **HAL**, est destinée au dépôt et à la diffusion de documents scientifiques de niveau recherche, publiés ou non, émanant des établissements d'enseignement et de recherche français ou étrangers, des laboratoires publics ou privés.

ANALYTICAL MODEL OF A WALL ACOUSTIC IMPEDANCE AND EXPERIMENTAL DATA

Béatrice Faverjon⁽¹⁾, Christian Soize⁽²⁾

⁽¹⁾Structural Dynamics and Coupled Systems Department, ONERA

E-mail:beatrice.faverjon@yahoo.fr

⁽²⁾Laboratoire de Mécanique, Université de Marne-La-Vallée

5 boulevard Descartes, 77454 Marne-La-Vallée, France. E-mail:soize@univ-mlv.fr

Abstract

Soundproofing schemes constituted of multilayer systems are used for acoustic insulation in many areas. In the context of the prediction of noise levels in vibroacoustic systems, numerical models are developed for the low and medium frequency ranges. Concerning models, a three-dimensional finite element model can be used or a classical approximation consisting in modeling the multilayer system by an acoustic impedance can be used. This paper deals with a multilayer system constituted of a porous medium inserted between two thin plates. An experimental data basis was carried out from a vibroacoustic experiment performed by ONERA. In this paper, we present the boundary value problem consisting of 12 coupled partial differential equations with boundary conditions. We present the analytical method allowing the local acoustic impedance equivalent to this multilayer system to be constructed. This method consists in introducing the unbounded medium in the plane directions x_1 and x_2 associated with the bounded system. A two-dimensional space Fourier transform introducing the wave vector coordinates k_1 and k_2 is used. The third space coordinate x_3 relative to the finite thickness is preserved. For a given frequency and for k_1 and k_2 fixed, the boundary value problem in x_3 , constituted of 12 differential equations in x_3 whose coefficients depend on k_1 and k_2 , with boundary conditions, is solved. By inverse Fourier transform with respect to k_1 and k_2 , the local wall acoustic impedance is deduced. The method which is proposed is not usual. Finally, a comparison of the experimental results with theoretical calculations is presented. These experimental results have also been used to construct an algebraic model of this acoustic impedance.

INTRODUCTION

The noise reduction can be obtained by adding absorptive treatments such as multilayer systems constituted of one or several porous media. The presence of the added porous media introduces difficulties in the modeling of the multilayer system. Indeed, the porous media are composed of a fluid phase coupled with a solid phase. There are several publications which have increased the understanding of the behavior of porous media (for example, see [1-7]). The methods used to solve the boundary value problem for the vibroacoustics behavior of a multilayer system are often based either on the three dimensional finite element methods [8-12] which are limited to the low frequencies or the analytical methods [13-15] which are limited to medium- and high-frequency ranges and unfortunately limited to simple systems. In this paper, we present the construction of an equivalent acoustic impedance of such a multilayer system for the medium- and high-frequency ranges using an analytical approach. The multilayer considered is a three-dimensional open porous medium inserted between two thin plates. By hypothesis, this multi-

layer system is infinite in the (x_1, x_2) plane direction and is finite in the x_3 direction. From the boundary value problem of this multilayer system [16], a new boundary value problem in x_3 is constructed by using a Fourier transform in x_1 and x_2 . Then, the acoustic impedance matrix is obtained by inverse Fourier transform. An experiment [17-18] has been developed to validate the theory. Using this experiment, an algebraic model of the equivalent acoustic impedance was developed and presented in [18]. In this paper, we present the boundary value problem using an isotropic model for each medium and we compare the numerical results with the experimental results.

EQUATIONS OF THE MULTILAYER SYSTEM IN FOURIER SPACE

The modeling of the open porous media is based on the Biot poroelasticity equations [2,4,5]. Concerning the two plates, denoted by P_1 and P_2 , the theory of Love-Kirchhoff with membrane motions is used. The multilayer system is considered as infinite in (x_1, x_2) as presented in figure 1. The coordinates (x_1, x_2, x_3) of a point belonging to the porous medium are given in the cartesian system whose origin belongs to the reference-plane S of the multilayer system which is chosen as the coupling interface Σ_1 . The x_3 coordinate of the coupling interface Σ_1 (or Σ_2) is 0 (or H) (in which H is the thickness of the porous medium). The two-dimensional Fourier transform in $\mathbf{x} = (x_1, x_2)$ is defined by

$$\begin{aligned} g(\mathbf{k}, \omega) &= \int_{\mathbb{R}^2} e^{i\mathbf{k}\cdot\mathbf{x}} g(\mathbf{x}, \omega) d\mathbf{x}, \\ g(\mathbf{x}, \omega) &= \frac{1}{(2\pi)^2} \int_{\mathbb{R}^2} e^{-i\mathbf{k}\cdot\mathbf{x}} g(\mathbf{k}, \omega) d\mathbf{k}, \end{aligned} \quad (1)$$

in which the wave vector is $\mathbf{k} = (k_1, k_2)$ and ω is the angular frequency.

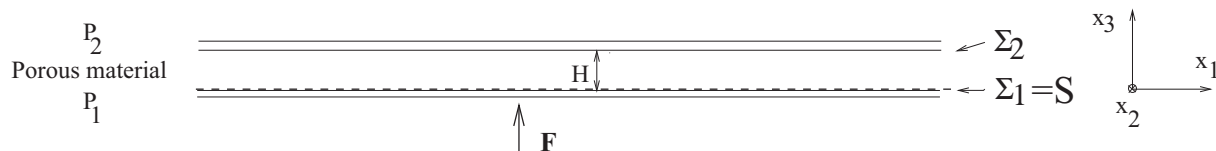


Figure 1. Multilayer system infinite in the (x_1, x_2) plane direction. The x_3 direction is finite.

The two-dimensional spatial Fourier transform of the dynamical equations of the porous medium is written as

$$\begin{aligned} -\omega^2 \rho_{11} u_i^s - \omega^2 \rho_{12} u_i^f - i\omega b (u_i^f - u_i^s) - \sigma_{ij,j}^s &= 0, \\ -\omega^2 \rho_{22} u_i^f - \omega^2 \rho_{12} u_i^s + i\omega b (u_i^f - u_i^s) - \sigma_{ij,j}^f &= 0. \end{aligned} \quad (2)$$

The first equation is related to the motion of the solid phase in the porous medium and the second one to the motion of the fluid phase. Let \mathbf{u}^s , $\mathbf{\sigma}^s$ and \mathbf{u}^f , $\mathbf{\sigma}^f$ be the Fourier transform of the displacements and of the stress tensors corresponding to the solid and the fluid phases, respectively. Since the porous medium is considered as isotropic, the permeability tensor, corresponding to the viscous effects, is reduced to a scalar denoted by b . The mass densities ρ_{11} , ρ_{22} and ρ_{12} correspond to the solid, to the fluid and to the coupling mass densities. The Fourier transform of the constitutive equation of the solid phase of the porous medium is given by

$$\begin{aligned}
\sigma_{11}^s &= A_F (-i k_1 u_1^s - i k_2 u_2^s + u_{3,3}^s) + B_F (-i k_1) u_1^s + C_F (-i k_1 u_1^f - i k_2 u_2^f + u_{3,3}^f), \\
\sigma_{22}^s &= A_F (-i k_1 u_1^s - i k_2 u_2^s + u_{3,3}^s) + B_F (-i k_2) u_2^s + C_F (-i k_1 u_1^f - i k_2 u_2^f + u_{3,3}^f), \\
\sigma_{33}^s &= A_F (-i k_1 u_1^s - i k_2 u_2^s + u_{3,3}^s) + B_F u_{3,3}^s + C_F (-i k_1 u_1^f - i k_2 u_2^f + u_{3,3}^f), \\
\sigma_{12}^s &= \sigma_{21}^s = \frac{-i B_F}{2} (k_2 u_1^s + k_1 u_2^s) \quad , \quad \sigma_{13}^s = \sigma_{31}^s = \frac{B_F}{2} (u_{1,3}^s - i k_1 u_3^s), \\
\sigma_{23}^s &= \sigma_{32}^s = \frac{B_F}{2} (u_{2,3}^s - i k_2 u_3^s), \tag{3}
\end{aligned}$$

in which $A_F = (1+i\omega a_1) \nu E / ((1+\nu)(1-2\nu)) + M(B-\Phi)^2$, $B_F = (1+i\omega a_1) E / (1+\nu)$ and $C_F = \Phi M(B-\Phi)$. The physical parameters of the solid phase are the Young modulus E , the Poisson ratio ν and the damping coefficient η such as $\eta = \omega a_1$. The porosity is denoted by Φ , and M and B are the Biot modulus and the coupling factor respectively. The Biot modulus is such that $M(\omega) = K_e(\omega) / \Phi$ in which $K_e(\omega)$ is the complex bulk modulus of air in the porous medium [4]. The Fourier transform of the constitutive equation of the fluid phase of the porous medium is written as

$$\sigma_{ii}^f = E_F (-i k_1 u_1^f - i k_2 u_2^f + u_{3,3}^f) + C_F (-i k_1 u_1^s - i k_2 u_2^s + u_{3,3}^s) \quad , \quad i = 1 \text{ to } 3, \tag{4}$$

in which E_F is defined by $E_F = \Phi^2 M$.

For plates P_1 and P_2 , the two-dimensional spatial Fourier transform of the dynamical equations are written as

$$\begin{aligned}
-\omega^2 \rho_{P_1} h_{P_1} \mathbf{u}^{P_1} + (1 + i\omega a_1^{P_1}) \mathbb{K}_1 \mathbf{u}^{P_1} &= \mathbf{F}_1 + \mathbf{f}(\omega), \\
-\omega^2 \rho_{P_2} h_{P_2} \mathbf{u}^{P_2} + (1 + i\omega a_1^{P_2}) \mathbb{K}_2 \mathbf{u}^{P_2} &= \mathbf{F}_2, \tag{5}
\end{aligned}$$

in which $\mathbf{u}^{P_r} = (v_1^{P_r}, v_2^{P_r}, w^{P_r})$ is the displacement field of plate P_r with $r = 1, 2$, ρ_{P_r} its mass density, h_{P_r} its thickness, $a_1^{P_r}$ its structural damping. The stiffness matrices \mathbb{K}_r with $r = 1, 2$ are given by

$$\mathbb{K}_r = \begin{bmatrix} \frac{D_{P_r}^m}{2} [(1+\nu^{P_r})k_1^2 + (1-\nu^{P_r})(k_1^2+k_2^2)] & \frac{D_{P_r}^m}{2} (1+\nu^{P_r})k_1k_2 & 0 \\ \frac{D_{P_r}^m}{2} (1+\nu^{P_r})k_1k_2 & \frac{D_{P_r}^m}{2} [(1+\nu^{P_r})k_2^2 + (1-\nu^{P_r})(k_1^2+k_2^2)] & 0 \\ 0 & 0 & D_{P_r}^f (k_1^2+k_2^2)^2 \end{bmatrix}, \tag{6}$$

in which $D_{P_r}^m = E^{P_r} h_{P_r} / (1 - (\nu^{P_r})^2)$, $D_{P_r}^f = E^{P_r} h_{P_r}^3 / (12 (1 - (\nu^{P_r})^2))$ and E^{P_r} , ν^{P_r} are the Young modulus and the Poisson ratio of plate P_r . Vectors \mathbf{F}_1 and \mathbf{F}_2 , correspond to the forces induced by the porous medium to plates P_1 and P_2 respectively, and are such that

$$\mathbf{F}_1 = \begin{bmatrix} \sigma_{13}^s(0) \\ \sigma_{23}^s(0) \\ \sigma_{33}^s(0) + \sigma_{33}^f(0) - i \frac{h_{P_1}}{2} (k_1 \sigma_{13}^s(0) + k_2 \sigma_{23}^s(0)) \end{bmatrix},$$

$$\mathbf{F}_2 = \begin{bmatrix} -\sigma_{13}^s(H) \\ -\sigma_{23}^s(H) \\ -\sigma_{33}^s(H) - \sigma_{33}^f(H) - i \frac{h_{P_2}}{2} (k_1 \sigma_{13}^s(H) + k_2 \sigma_{23}^s(H)) \end{bmatrix}. \quad (7)$$

The experiment described in [17,18] gives measurements of the acoustic impedance of the multilayer system. In the experiment, the multilayer system is finite in plane directions, whereas, for the medium- and high frequencies, the analytical model uses an infinite multilayer system in plane directions which is associated with the finite multilayer system of the experiment. Normal point forces are successively applied to the 25 points in plate P_1 defined in figure 2. The measured responses are the normal accelerations at the 25 points in plate P_1 and at the corresponding 25 points in plate P_2 . The 25 points on plate P_2 are directly above the 25 points on plate P_1 . The 25×25 impedance matrix is deduced for which each term is equal to the ratio of the normal point force with the difference between the normal velocities to plates P_1 and P_2 . In order to validate the analytical model, normal point forces are used as input instead of a pressure field. Each medium is homogeneous and isotropic in (x_1, x_2) plane. Then, the impedance matrix is constructed by using an analytical approach for which point forces are successively applied to 25 points of the mesh defined in figure 2, similarly to the experiment. We then have $\mathbf{f}(\omega) = (0, 0, f(\omega))$ in equation Eq. (5) in which the modulus $f(\omega)$ is such that $p(\mathbf{x}, \omega) = f(\omega) \delta_0(\mathbf{x})$ with δ_0 the Dirac function.

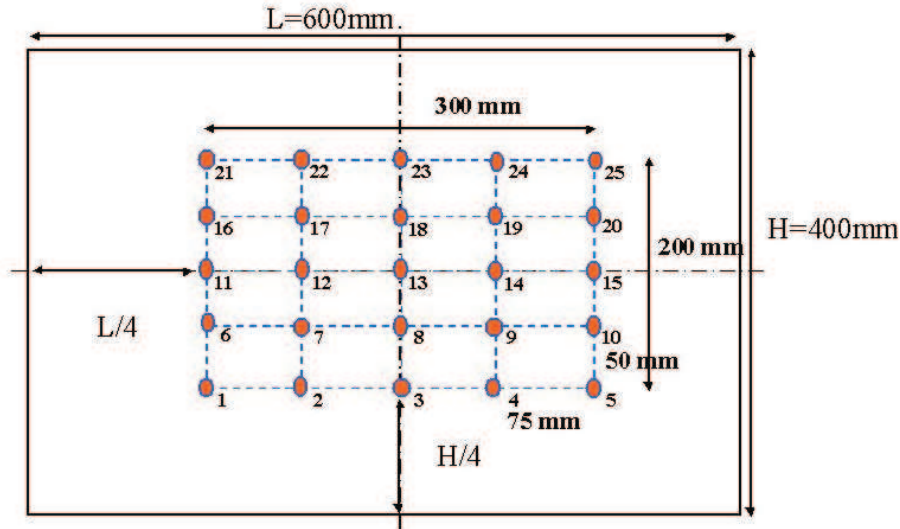


Figure 2. Position of the 25 measure points in plate P_1 and in the corresponding 25 points in plate P_2 .

Finally, the two-dimensional spatial Fourier transform of the boundary conditions on the interfaces between the two plates and the porous layer are written as

$$\begin{aligned}
u_\alpha^s &= v_\alpha^{P_1} + i \frac{h_{P_1}}{2} k_\alpha w^{P_1} \quad , \quad u_3^s = w^{P_1} \quad , \quad u_3^f = w^{P_1} \quad , \quad \text{on } \Sigma_1 \quad , \quad \alpha = 1, 2 \quad , \\
u_\alpha^s &= v_\alpha^{P_2} - i \frac{h_{P_2}}{2} k_\alpha w^{P_2} \quad , \quad u_3^s = w^{P_2} \quad , \quad u_3^f = w^{P_2} \quad , \quad \text{on } \Sigma_2 \quad . \quad (8)
\end{aligned}$$

Equations Eqs. (2) to (8) define the boundary value problem of the multilayer system formulated in variables k_1 , k_2 and x_3 .

EXPRESSION OF THE EQUIVALENT ACOUSTIC IMPEDANCE

The boundary value problem constructed in Section 2 is constituted of 12 coupled differential equations in x_3 with boundary conditions, whose coefficients depend on ω and \mathbf{k} . The impedance density function $z(\mathbf{x} - \mathbf{x}', \omega)$ is such that [18]

$$p(\mathbf{x}, \omega) = \int_{\mathbf{x}' \in S} z(\mathbf{x} - \mathbf{x}', \omega) \Delta v(\mathbf{x}', \omega) dS_{\mathbf{x}'} \quad , \quad (9)$$

in which \mathbf{x} and \mathbf{x}' are the position of the normal point force and the measurement point in the reference-plane S and where $dS_{\mathbf{x}'}$ is the area measure. The difference $\Delta v(\mathbf{x}', \omega)$ of the normal velocities at point \mathbf{x}' is given by $\Delta v(\mathbf{x}', \omega) = v^{P_1}(\mathbf{x}', \omega) - v^{P_2}(\mathbf{x}', \omega)$ where, for $r = 1, 2$, $v^{P_r}(\mathbf{x}', \omega)$ is the normal velocity to plate P_r . The space Fourier transform of Eq. (9) is written as

$$p(\mathbf{k}, \omega) = i \omega z(\mathbf{k}, \omega) \Delta w(\mathbf{k}, \omega) \quad , \quad (10)$$

in which $\Delta w(\mathbf{k}, \omega) = w^{P_1}(\mathbf{k}, \omega) - w^{P_2}(\mathbf{k}, \omega)$ is the Fourier transform of the difference $\Delta w(\mathbf{x}, \omega) = w^{P_1}(\mathbf{x}, \omega) - w^{P_2}(\mathbf{x}, \omega)$ of the normal displacements at point \mathbf{x} . Solving the boundary value problem in x_3 allows an equation relating $f(\omega)$ and $\Delta w(\mathbf{k}, \omega)$ to be constructed. Substituting the Fourier transform of the constitutive equations into the Fourier transform of the dynamical equations of the plates yields an equation between the plate displacements, the porous-medium displacements and the normal point force. Substituting the Fourier transform of the constitutive equations of the porous medium into the Fourier transform of its dynamical equations and using the Fourier transform of the boundary conditions, allows the displacements of the porous medium to be eliminated in $x_3 = 0$ and $x_3 = H$ [16]. Such a method is not self evident due to the conditioning problems, and special developments have been carried out [16]. The matrix of the porous medium has eight eigenvalues and the conditioning problems are due to four eigenvalues whose real part are positive. Finally, the Fourier transform of the dynamical equations of the two plates can be rewritten as

$$\mathbb{A}^P \mathbf{u}^P = \mathbf{F} + \mathbf{F}^e \quad , \quad (11)$$

in which \mathbb{A}^P , \mathbf{F} and \mathbf{F}^e are defined below. The matrix \mathbb{A}^P is defined by $\mathbb{A}^P = \begin{bmatrix} \mathbb{A}^{P_2} & 0 \\ 0 & \mathbb{A}^{P_1} \end{bmatrix}$ in which \mathbb{A}^{P_1} and \mathbb{A}^{P_2} are given by

$$\begin{aligned}
\mathbb{A}^{P_1} &= -\omega^2 \rho_{P_1} h_{P_1} \mathbf{u}^{P_1} + (1 + i \omega a_1^{P_1}) \mathbb{K}_1 \mathbf{u}^{P_1} \quad , \\
\mathbb{A}^{P_2} &= -\omega^2 \rho_{P_2} h_{P_2} \mathbf{u}^{P_2} + (1 + i \omega a_1^{P_2}) \mathbb{K}_2 \mathbf{u}^{P_2} \quad . \quad (12)
\end{aligned}$$

The external normal point force is denoted by \mathbf{F}^e such that $\mathbf{F}^e = (0, \mathbf{f})$. From the eliminating process described above, the force $\mathbf{F} = (\mathbf{F}_2, \mathbf{F}_1)$ induced by the porous medium to the two plates is written as

$$\mathbf{F} = \mathbb{N}(\mathbf{k}, \omega) \mathbf{u}^P, \quad (13)$$

in which $\mathbb{N}(\mathbf{k}, \omega)$ is a complicated expression detailed in reference [16]. Substituting Eq. (13) into Eq. (11), yields

$$\mathbf{u}^P(\mathbf{k}, \omega) = \mathbb{M}^{-1}(\mathbf{k}, \omega) \mathbf{F}^e(\omega) \quad \text{with} \quad \mathbb{M}(\mathbf{k}, \omega) = \mathbb{A}^P(\mathbf{k}, \omega) - \mathbb{N}(\mathbf{k}, \omega), \quad (14)$$

which can be rewritten as

$$\Delta w(\mathbf{k}, \omega) = h(\mathbf{k}, \omega) f(\omega) \quad \text{with} \quad h(\mathbf{k}, \omega) = [\mathbb{M}^{-1}(\mathbf{k}, \omega)]_{66} - [\mathbb{M}^{-1}(\mathbf{k}, \omega)]_{36}. \quad (15)$$

From Eq. (15), we deduce that

$$\Delta w(\mathbf{x}, \omega) = \int_{\mathbb{R}^2} h(\mathbf{x} - \mathbf{x}', \omega) p(\mathbf{x}', \omega) d\mathbf{x}'. \quad (16)$$

Since $p(\mathbf{x}, \omega) = f(\omega) \delta_0(\mathbf{x})$ and $f(\omega) = 1$ (experimental value), we obtain

$$\Delta w(\mathbf{x}, \omega) = h(\mathbf{x}, \omega) \quad \text{with} \quad h(\mathbf{x}, \omega) = \frac{1}{(2\pi)^2} \int_{\mathbb{R}^2} e^{-i\mathbf{k}\cdot\mathbf{x}} h(\mathbf{k}, \omega) d\mathbf{k}. \quad (17)$$

Since the media are isotropic in (x_1, x_2) plane, we have

$$\begin{aligned} h(\mathbf{k}, \omega) &= h(k, \omega) \quad , \quad \Delta w(\mathbf{k}, \omega) = \Delta w(k, \omega) \quad , \quad \text{in which} \quad k = \|\mathbf{k}\| \quad , \\ h(\mathbf{x}, \omega) &= h(r, \omega) \quad , \quad \Delta w(\mathbf{x}, \omega) = \Delta w(r, \omega) \quad , \quad \text{in which} \quad r = \|\mathbf{x}\| \quad , \end{aligned} \quad (18)$$

and consequently,

$$\Delta w(r, \omega) = \frac{1}{2\pi} \int_0^{+\infty} k J_0(kr) h(k, \omega) dk, \quad (19)$$

in which $J_0(kr)$ is the zero-order Bessel function. This equation gives a continuous expression of the normal displacement due to a normal point excitation located at origin 0. Since the experimental impedance matrix is constructed for 25 point forces, in order to validate the analytical model, we use a similar construction. Let $[\Delta W(\omega)]$ be the complex matrix whose elements are such that $[\Delta W(\omega)]_{jk} = \Delta w(r_{jk}, \omega)$ in which $r_{jk} = \|M_j M_k\|$ is the distance between the driving point M_k and the receiving point M_j located at the nodes of the mesh defined in figure 2, and where $\Delta w(r, \omega)$ is calculated with Eq. (19). The associated impedance matrix is then written as

$$[Z^{mod}(\omega)] = \frac{1}{i\omega} [\Delta W(\omega)]^{-1}. \quad (20)$$

In Eq. (19), the integral is calculated numerically using adapted approximation.

NUMERICAL RESULTS AND EXPERIMENTAL COMPARISONS

Physical parameters of the materials. The multilayer system is constituted of two isotropic aluminium plates P_1 and P_2 , whose thickness are $h_{P_1} = 1$ mm and $h_{P_2} = 3$ mm, and of a polyurethan foam which is modeled by an isotropic viscoelastic open porous medium saturated in air. Physical parameters of both plates are given in table 1.

Parameter	Value
Young modulus E^P (Pa)	$7.4 \cdot 10^{10}$
Poisson ratio ν^P	0.33
Damping factor η^P	10^{-4}
Mass density ρ^P ($\text{kg}\cdot\text{m}^{-3}$)	2800

Table 1. Physical parameters for plates P_1 and P_2 .

Since the fluid phase of the porous medium is air, we use the usual parametric values for air. Concerning the solid phase, its physical parameters and the coupling parameters between the two phases are given in table 2.

Parameter	Value
Mass density ρ_1 ($\text{kg}\cdot\text{m}^{-3}$)	34.2
Young modulus E (Pa)	110000
Shear modulus G (Pa)	$\frac{E}{2(1+\nu)}$
Damping factor η_s	0.09
Poisson ratio ν	0.35
Porosity Φ	0.96
Tortuosity α	1.27
Resistivity σ ($\text{N}\cdot\text{s}\cdot\text{m}^{-4}$)	10867
Viscous characteristic length Λ (μm)	96
Thermal characteristic length Λ' (μm)	288

Table 2. Solid phase parameters and fluid-solid coupling parameters for the porous medium.

Local acoustic impedance. The local acoustic impedance corresponds to the impedance from one point on P_1 to another point on P_2 , directly over the point in P_1 and is given by the diagonal terms multiplied by an adapted elementary surface of the impedance matrix defined by Eq. (20) [18]. For two points 8 and 16, figures 3 and 4 display the analytical model of the local impedance (solid line) as a function of the frequency and compared with the experimental results (dash line).

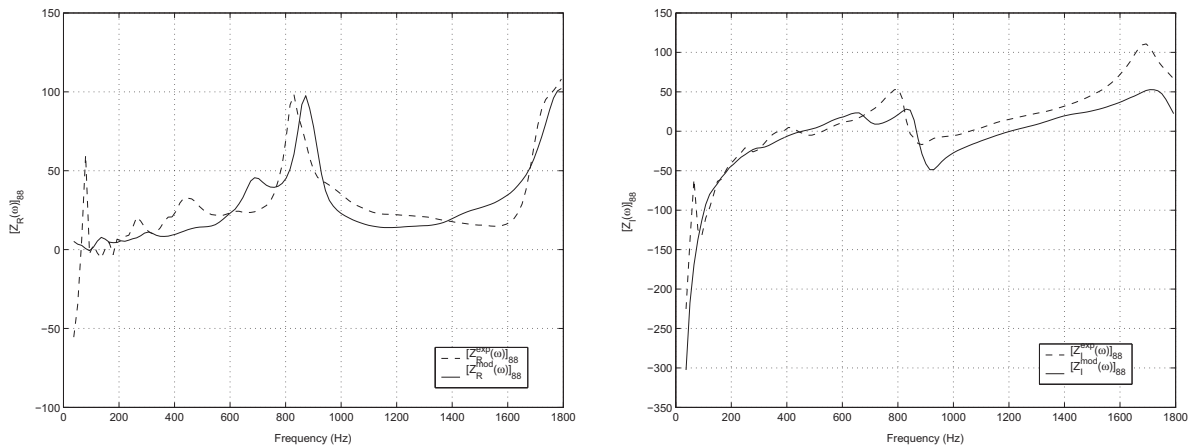


Figure 3. Local acoustic impedance at point 8. Real part on the left, imaginary part on the right. Analytical model (solid line), experimental results (dash line).

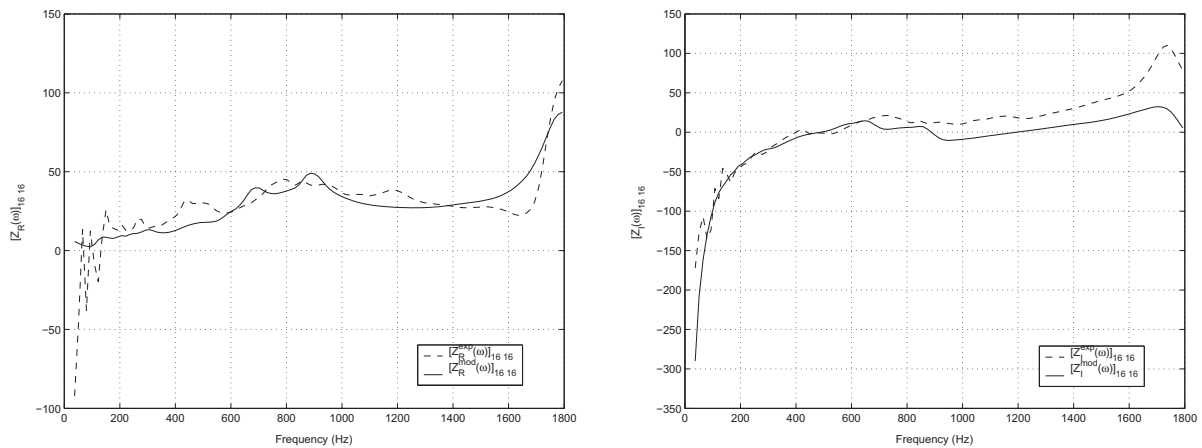


Figure 4. Local acoustic impedance at point 16. Real part on the left, imaginary part on the right. Analytical model (solid line), experimental results (dash line).

For these two points, the analytical model is very close to the experimental results. For the other points, the quality of the comparisons is similar. In addition, since the diagonal terms are similar, an averaging over the diagonal terms is performed. Figure 5 shows this averaging for the analytical local impedance and for the experiment local impedance. There is again a good agreement between analytical and experimental results.

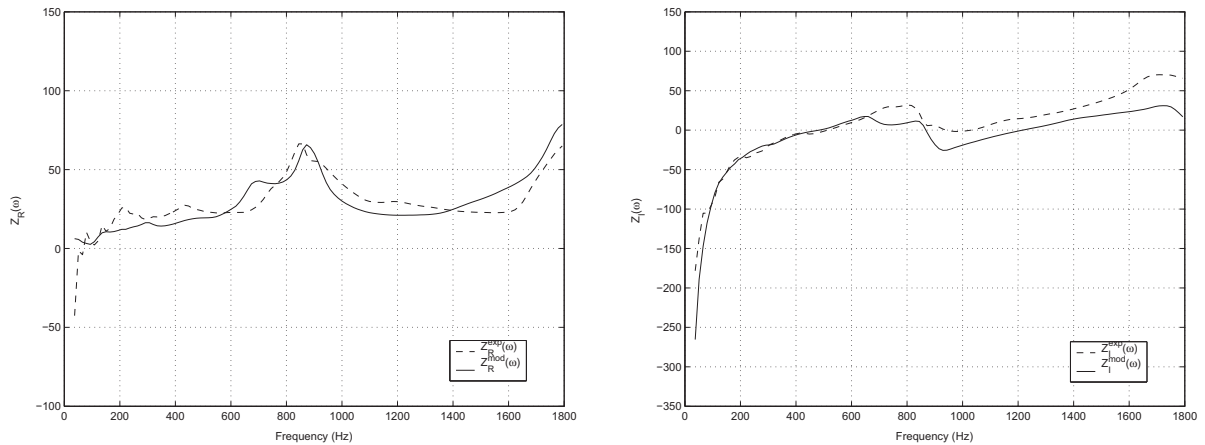


Figure 5. Average local acoustic impedance. Real part on the left, imaginary part on the right. Analytical model (solid line), experimental results (dash line).

Cross acoustic impedance. The acoustic impedance of the multilayer system is local for frequencies larger than 300 Hz [16,18]. The cross acoustic impedance corresponds to the transfert impedance from one point on P_1 to another point on P_2 , not directly over the point in P_1 . The aspect of these transfert impedances, given by the off-diagonal terms of the impedance matrix, as a function of the distance r is an exponential decreasing function with r , as it can be seen in figures 6 to 9. Figures 6 and 7 correspond to frequency 500 Hz and figures 8 and 9 to frequency 1400 Hz. Figures 6 and 8 display all the off-diagonal terms of the real part and imaginary part of the impedance matrix (circles correspond to the analytical model and crosses to the experimental data), as functions of the distance r . It should be noted that, for the imaginary part, there is an additional phase for $r = 0$ depending on the frequency [16,18]. Figures 7 and 9 display the average values of these off-diagonal terms at the same distance r .

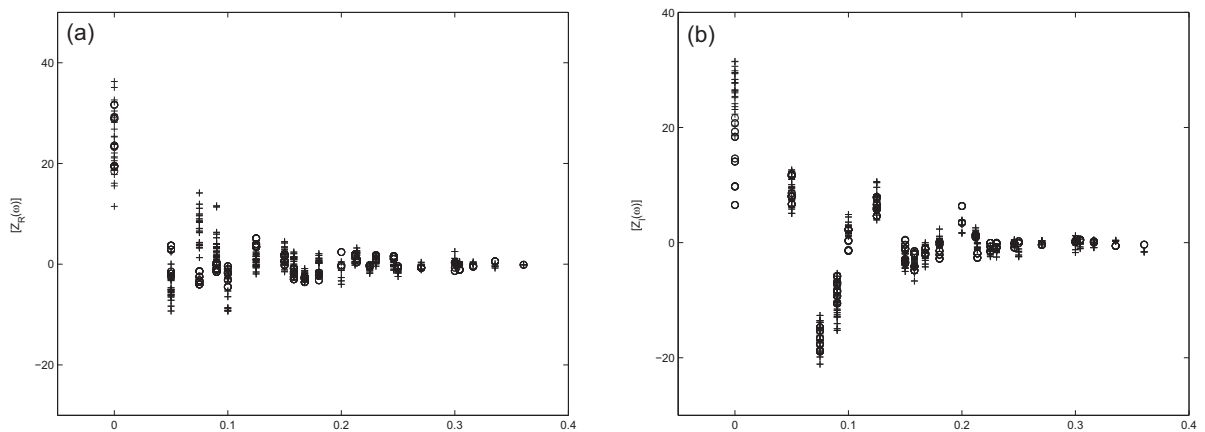


Figure 6. Off-diagonal terms of the acoustic impedance matrix as a function of distance r at 500 Hz. Analytical model (circle), experimental results (cross). Real part on the left, imaginary part on the right.

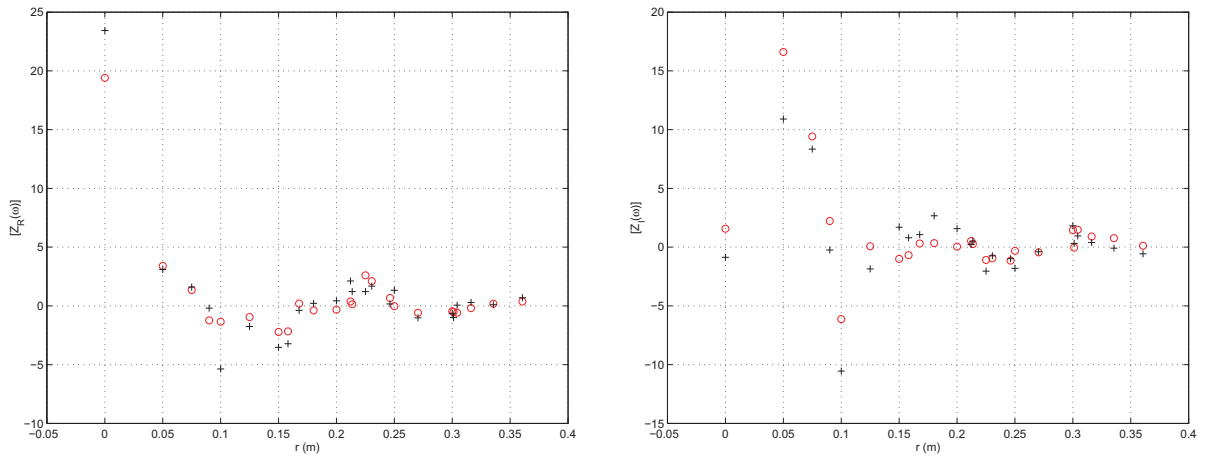


Figure 7. Average of all the off-diagonal terms of the acoustic impedance matrix at the same distance r , function of distance r , at 500 Hz. Analytical model (circle), experimental results (cross). Real part on the left, imaginary part on the right.

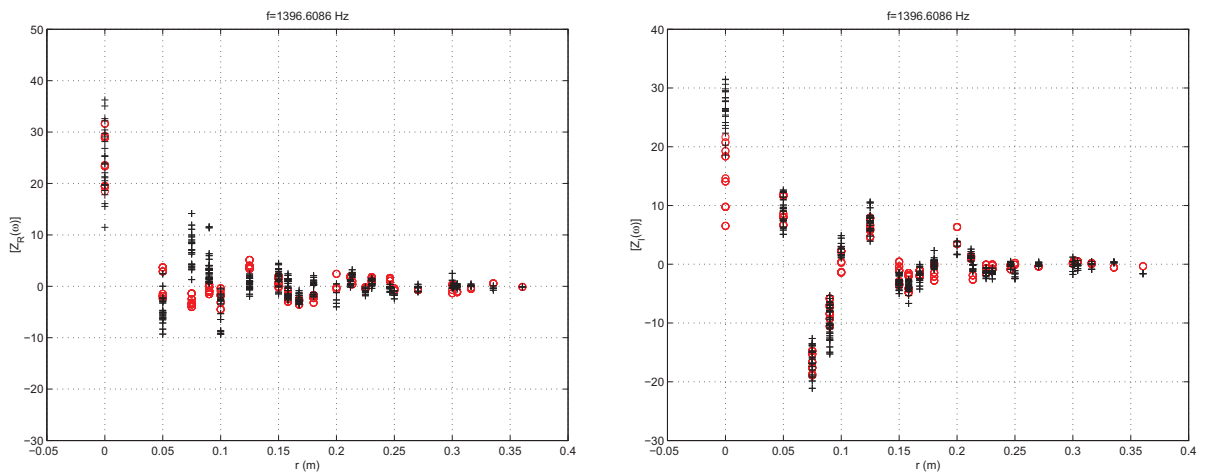


Figure 8. Off-diagonal terms of the acoustic impedance matrix as a function of distance r at 1400 Hz. Analytical model (circle), experimental results (cross). Real part on the left, imaginary part on the right.

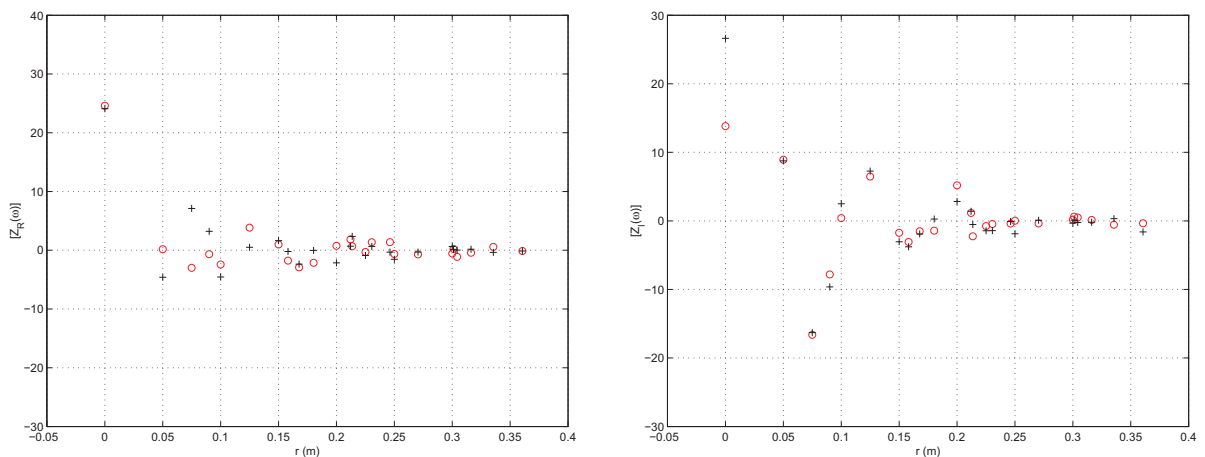


Figure 9. Average of all the off-diagonal terms of the acoustic impedance matrix at the same distance r , function of distance r , at 1400 Hz. Analytical model (circle), experimental results (cross). Real part on the left, imaginary part on the right.

CONCLUSIONS

This paper presents the construction of an equivalent acoustic impedance for a multilayer system constituted of a porous medium inserted between two thin plates. The boundary value problem is solved by using a spectral approach. Validation is obtained by comparing theoretical predictions with experimental results in the medium- and high-frequency ranges. The experimental comparisons are satisfactory for both the local acoustic impedance and the cross acoustic impedance.

REFERENCES

1. Zwikker, C. and Kosten, C.W., *Sound Absorbing Materials*, Elsevier, New York, 1949.
2. Biot, M.A., *Acoustics, Elasticity and Thermodynamics of Porous Media : Twenty one papers by M.A. Biot*, ed. I. Tolstoy, Acoustical Society of America, New York, 1992.
3. Delany, M.E. and Bazley, E.N., Acoustical properties of fibrous materials, *Appl. Acoustics*, 1970, **3**, 105-116.
4. Allard, J.F., Aknine, A. and Depollier, C., Acoustical properties of partially reticulated foams with high and medium flow resistance, *J. Acoust. Soc. Am.*, 1986, **79** (6), 1734-1740.
5. Coussy, O., *Mécanique des milieux poreux*, Technip, Paris, 1991.
6. Bourbié, T., Coussy, O. and Zinszner, B., *Acoustics of porous media*, Technip, Paris, 1987.
7. Johnson, D.L., Koplik, J. and Dashen, R., Theory of dynamic permeability and tortuosity in fluid-saturated porous media, *J. Fluid Mechanics*, 1987, **176**, 379-402.
8. Atalla, N., Panneton, R. and Debergue, P., A mixed displacement-pressure formulation for poroelastic materials, *J. Acoust. Soc. Am.*, 1998, **104** (3), 1444-1452.
9. Panneton, R. and Atalla, N., An efficient finite element scheme for solving the three-dimensional poroelasticity problem in acoustics, *J. Acoust. Soc. Am.*, 1997, **101** (6), 3287-3298.
10. Sgard, F.C., Atalla, N. and Nicolas, J., A numerical model for the low-frequency diffuse field sound transmission loss of double-wall sound barriers with elastic porous linings, *J. Acoust. Soc. Am.*, 2000, **108** (6), 2865-2872.
11. Kang, Y.J. and Bolton, J.S., A finite element model for sound transmission through foam-lined double panel structures, *J. Acoust. Soc. Am.*, 1996, **99**, (5), 2755-2765.
12. Göransson, P., A 3-D, symmetric, finite element formulation of the Biot equations with applications to acoustic wave propagation through an elastic porous medium, *Int. J. Num. Meth. Eng.*, 1998, **41**, 167-192.
13. Allard, J.F., Champoux, Y. and Depollier, C., Modelization of layered sound absorbing materials with transfert matrices, *J. Acoust. Soc. Am.*, 1987, **82** (5), 1792-1796.
14. Lauriks, W., Mees, P. and Allard, J.F., The acoustic transmission through layered systems, *J. Sound Vib.*, 1992, **155** (1), 125-132.
15. Bolton, J.S., Shiau, N.M. and Kang, Y.J., Sound transmission through multi-panel structures lined with elastic porous materials, *J. Sound Vib.*, 1996, **191** (3), 317-347.
16. Faverjon, B., Modélisation et validation expérimentale d'un modèle d'impédance acoustique dans le domaine des moyennes et hautes fréquences pour un système

- multicouche composé d'un matériau poreux épais inséré entre deux plaques minces, Doctorate thesis, Conservatoire National des Arts et Métiers, Paris (in progress)
17. Guillaumie, L., Wall acoustic impedance. Experimental identification, Report n0 RTS 2/03239 Structural Dynamics and coupled Systems Department, ONERA, Paris, 2001 (in french).
 18. Faverjon, B. and Soize, C., Algebraic model of a wall acoustic impedance constructed using experimental data, International Conference on Noise and Vibration Engineering, ISMA 2002, Leuven, September 16-18, 2002.